Final Report

BASIC FACTORS CONTROLLING PEST IN HIGH TEMPERATURE SYSTEMS

to

NATIONAL AERONAUTICS AND SPACE ADMINISTRATION
WASHINGTON, D. C. 20546

CONTRACT NO. NASW-1887

NOVEMBER 20, 1971

Arthur D. Little, Inc.

FINAL REPORT

Basic Factors Controlling Pest in High Temperature Systems

by

J. Berkowitz-Mattuck and M. Rossetti
Arthur D. Little, Inc.
Cambridge, Mass. 02140

Contract Number NASW-1887
National Aeronautics and Space Administration
Washington, D. C. 20546

November 20, 1971

TABLE OF CONTENTS

ACKNOWLEDGEMENTS

The authors are pleased to acknowledge the invaluable help of Dr. John Haggerty of Arthur D. Little, Inc. in preparing Section III of the manuscript. We are also indebted to Dr. Edward Peters for his assistance in interpreting the Laue X-ray patterns discussed in the report.

I. INTRODUCTION

The catastrophic disintegration in air at intermediate temperatures of refractory materials which are very resistant to oxidation at high temperatures is known in the literature as "pest." The phenomenon was first observed in molybdemum disilicide ($MoSi_2$), and was later found to be characteristic of the oxidation behavior of several chemically related non-cubic silicides, including Mo_5Si_3, WSi_2, and W_5Si_3. Berkowitz-Mattuck, Rossetti, and Lee[1] have shown that pest failure is $MoSi_2$ is due to stress-accelerated oxidation at the tips of Griffith flaws, leading to flaw growth and eventual material fracture. At sufficiently high temperatures where lattice deformation becomes significant, internal stresses are reduced and can no longer provide an important driving force for preferential oxidation. Thus, pest failure is typically limited to an intermediate temperature range.

Although pest failure in molybdenum and tungsten silicides bears a superficial resemblance to other solid state disintegration phenomena, the failure mechanism is fundamentally different. The "tin pest" for example, is a temperature sensitive phase change which, unlike the silicide pest, does not depend in any way on chemical interaction with the environment. Disintegration has been observed in the CsCl structure compounds AgMg, NiAl, and NiGa, but it is primarily intergranular and results from oxygen and nitrogen segregation[2] at grain boundaries. Pest disintegration is for the most part transgranular.

The intermediate temperature disintegration that has been reported in $CbAl_3$, $TaAl_3$, and $MoAl_3$ seems closely analogous to silicide pest. In $CbAl_3$, which has been studied most extensively, disintegration does only occur in the presence of air or oxygen, and it is primarily transgranular. The present program was undertaken to determine whether the mechanism proposed for pest failure in silicides might also be responsible for pest failure in $CbAl_3$. The aim was to correlate oxidation kinetics in the range where disintegration of $CbAl_3$ is observed with delayed failure data obtained under similar conditions. Since the fundamental importance of plastic deformation in mitigating the pest problem is well-recognized, studies were also undertaken to develop some understanding of deformation mechanisms in both silicides and aluminides.

II. THE PEST PHENOMENON IN $CbAl_3$

If the mechanism responsible for pest failure in $MoSi_2$ is also to account for intermediate temperature disintegration in $CbAl_3$, the analogous results are to be expected for certain delayed failure and weight change experiments. In particular, single crystals of $MoSi_2$ are not ordinarily subject to pest disintegration. The single crystals are subject to delayed failure, however, under the conditions of temperature and oxygen pressure that lead to pest in polycrystals. Furthermore, the delayed failure times for single crystals, at given stress levels, can be correlated with the times for onset of pest disintegration in polycrystals. A particularly striking result is the minimum observed at 500°C for both the time to initial disintegration in polycrystalline $MoSi_2$, and the time to failure in single crystalline $MoSi_2$ at a given stress level.

Disintegration of polycrystalline $CbAl_3$ in air has been observed at all temperatures between 540° and 850°C. In early work on arc-melted samples, disintegration appeared to be most rapid at 750°C. Later work at Arthur D. Little, Inc. on zone melted samples indicated monotonically increasing rates of disintegration with temperature over the entire pest range. Excellent oxidation resistance, with the formation of a tightly adherent α-Al_2O_3 protective scale, has been reported at temperatures in the range 900-1100°C. No data are available on single crystal $CbAl_3$.

A. Materials Preparation

Polycrystalline boules of columbium aluminide were pulled from a melt by the Czochralski growth technique. The melt was prepared by reacting high purity aluminum (99.997%) and columbium (99.9%) in a pyrolytic boron nitride crucible. A charge of approximately 60 grams was used and consisted of short lengths, approximately one inch, of 1/4 inch columbium rod and one piece of aluminum of the appropriate weight. Prior to placement in the crucible, the surfaces of the columbium rod were ground with 400 grit silicon carbide paper then washed and

rinsed in methanol using ultrasonic action. The rods were stored under methanol until ready for loading into a crucible. The aluminum surfaces were cleaned and stored similarly. Each crucible charge contained 2% excess aluminum to compensate for evaporative losses during growth.

Prior to the actual growth run, the crucible charge was melted under a 70 psig argon atmosphere and allowed to react. The melt was then cooled and removed from the crucible. The outer surfaces of the resultant ingot were ground with silicon carbide paper to remove minor amounts of columbium oxide. The ingot was then broken into several pieces, loaded back into the crucible and remelted. Both the elemental and pre-reacted charges were melted by radiation from an inductively heated graphite susceptor surrounding the boron nitride crucible.

For the crystal growth runs, a 1/16" diameter boron nitride rod was used as a starting seed. Crack-free polycrystalline boules proved extremely difficult to prepare. While pyrolytic boron nitride was the best crucible material found, it did not appear to be entirely inert. During growth copious amounts of aluminum vapor escape from the melt and find their way back to the melt surface as aluminum oxide in spite of the high pressure, high purity argon atmosphere. The oxide scum limits the actual time of the growth runs. The oxide grains act as nucleating sites for spurious grain growth which can and does lead to microcracking in the boules. With the pyrolytic boron nitride crucibles, using growth rates of about 1 inch per hour, we were able to obtain polycrystalline boules of columbium aluminide of sufficient crack-free length for delayed failure measurements.

Repeated attempts to grow single crystals of $CbAl_3$ were all unsuccessful. The initial runs were made with the melt contained in an aluminum oxide crucible. A sapphire light pipe was used as a seed crystal. The continuous generation of a mixed oxide scum on the melt surface, and copious smoking or evaporation from the melt precluded single crystal formation. The use of a pyrolytic boron nitrate crucible and a seed cut from a polycrystalline sample provided some degree of

improvement, however, scum formation was still too rapid to permit fabrication of crack-free single crystal boules of sufficient length and uniform base level strength for delayed failure experiments.

B. Delayed Failure of Polycrystalline $CbAl_3$

Rectangular bar specimens were cut from the as-grown polycrystalline boules with a spark discharge machine. The surfaces were ground on a 300 grit diamond-bonded abrasive wheel, then on successively finer silicon carbide laps down to 600 grit, and finally polished on a high speed 6μ diamond lap. The final size of the specimens was 0.1" x 0.08" x 5/8".

Base level tensile strengths, S_N, were measured at 625°C in vacuum. Three rectangular sample bars, selected at random from the cut polycrystalline boules, gave an average S_N of 31,400 $\pm$ 4800 psi.

Delayed failure experiments have been carried out in air at three temperatures, 625, 700, and 825°C, within the pest range for $CbAl_3$, and one temperature, 875°C, found to be outside the range in some experiments. Rectangular bars were four-point dead-weight leaded in tension at a fraction S/S_N of the base level strength. As oxidation proceeded, the $CbAl_3$ substrate weakened and eventually failed. The time to failure at 700°C, as indicated in Figure 1, is accelerated by the applied stress. At 625°C, where the rate of surface oxidation is less than at 700°C, a longer time is required for failure at a given S/S_N level. As expected on the basis of the weight change results presented below, delayed failure times continued to decrease with temperature at 825 and 875°C. From the Arrhenius plot shown in Figure 2, the activation energy for delayed failure of $CbAl_3$ in air is calculated to be 28.6 kcal/mole over the range of 625 to 875°C.

C. Weight Change of Polycrystalline $CbAl_3$ During Oxidation

A complete series of weight change vs. time curves made on zone refined columbium aluminide samples during oxidation at temperatures from 500 to 900°C in one atmosphere of oxygen is presented in Figures

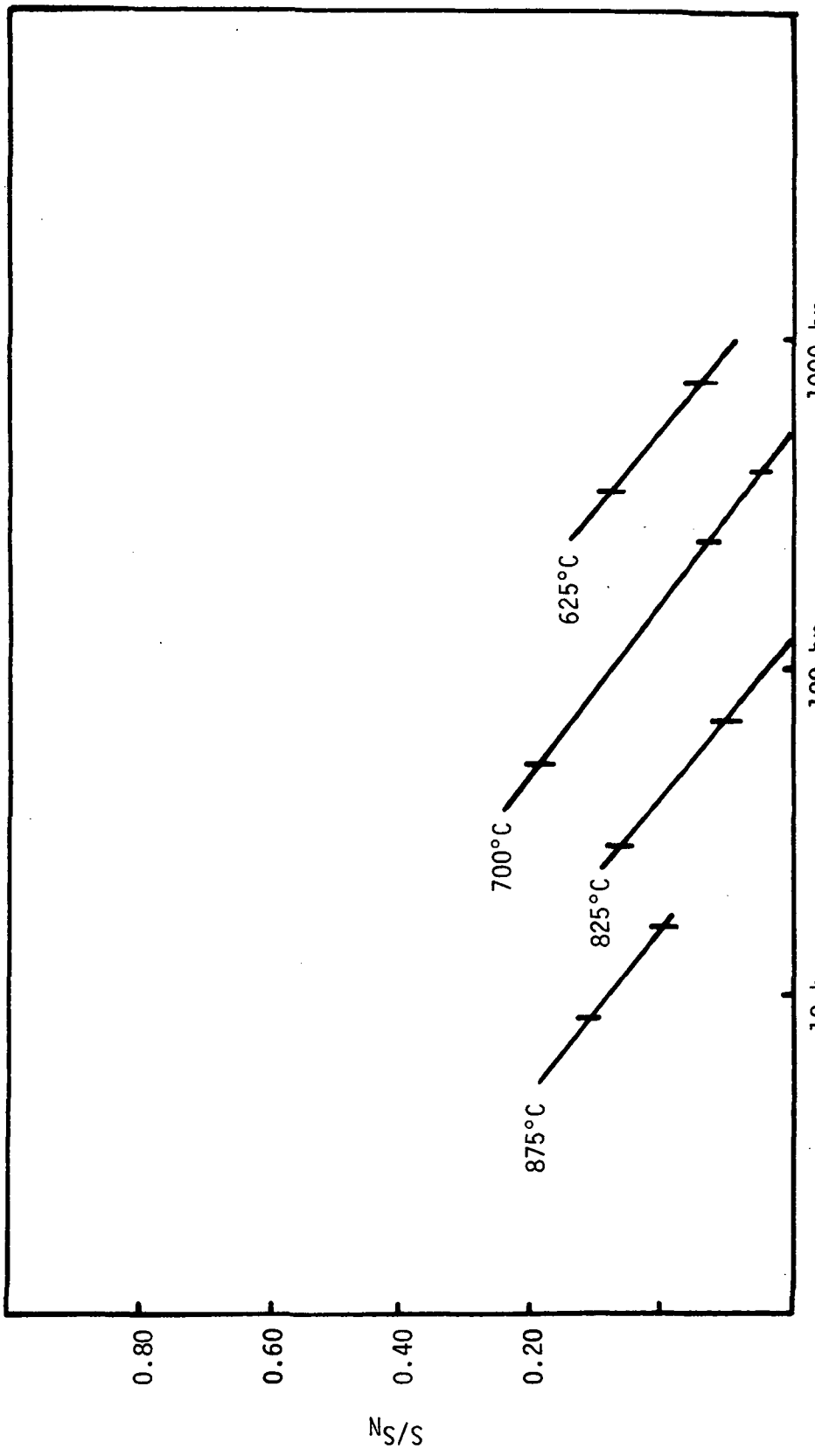

FIGURE 1 DELAYED FAILURE CURVES FOR POLYCRYSTALLINE $AbAl_3$ IN AIR AT VARIOUS TEMPERATURES

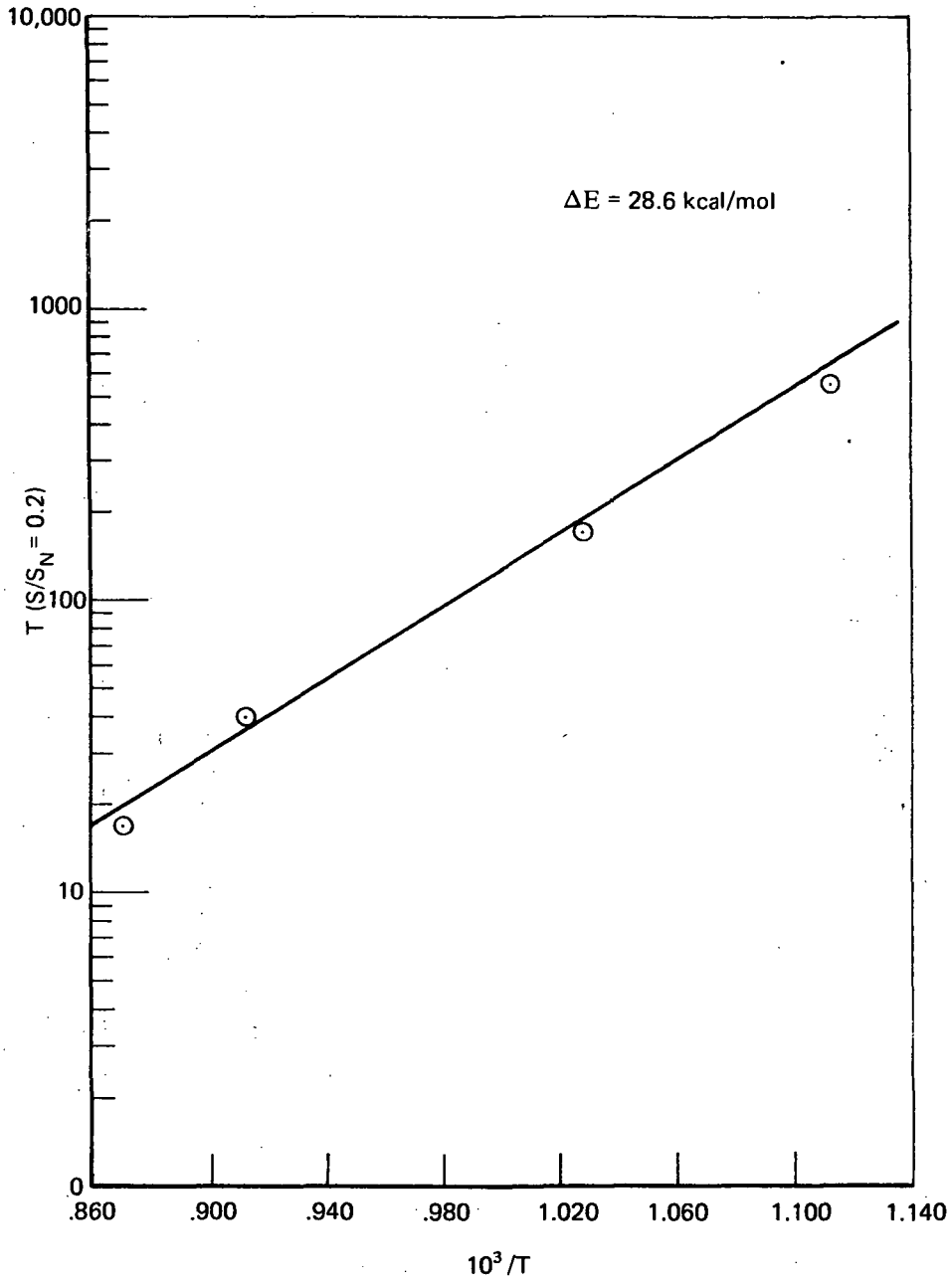

FIGURE 2 TEMPERATURE DEPENDENCE OF DELAYED FAILURE TIMES FOR $CbCl_3$ IN AIR AT $S/S_N = 0.2$

3 and 4. Between 500 and 850°C, the curves show an initial period of linear oxidation, followed by a period of continuously accelerating oxidation rate. The poor reproducibility of results at 800°C (see Figure 4) is due to variations in the number of cracks from sample to sample. The cracks were formed as a result of thermal stresses induced during cooling of the crystals from the melt.

At 900°C there is an abrupt change in the oxidation behavior. The rate of weight gain decreases continuously from the beginning indicating that a protective oxide has been formed. Oxidation was parabolic for the first two hours. Thereafter, the oxidation rate was even slower. After 20 hours, there was still no signs of pesting.

In Figure 5, the time of transition between the initial period of low linear oxidation rate and the later period of accelerating rate (induction time) is plotted as a function of temperature for the one atmosphere oxygen data. Unlike a similar plot for $MoSi_2$, which goes through a minimum at about 500°C, the induction time for $CbAl_3$ steadily decrease to 850°C. At 900°C, a totally different oxidation mechanism is initiated and $CbAl_3$ is no longer subject to pest. The temperature transistion from pesting to non-pesting behavior thus appears to be quite sharp.

Under the present program, the weight change behavior of $CbAl_3$ was measured in air at 700, 825, and 875°C. A simple apparatus was constructed incorporating a quartz helical spring balance as shown schematically in Figure 6. For each set of experimental conditions a single nugget of polycrystalline columbium aluminide weighing about 0.15g was contained in an open platinum bucket, which was attached to the quartz spring by a 0.003" diameter platinum wire. The assembly was contained in a 1" I.D. quartz tube upon which a reference line was inscribed. The lower part of the quartz tube was surrounded by a kanthal resistance heated furnace. Temperature measurements were made using a Pt/Pt 10% Rd thermocouple. Weight gains were then monitored as a function of time by following spring displacement relative to the reference line with a cathetometer. The spring had a sensitivity

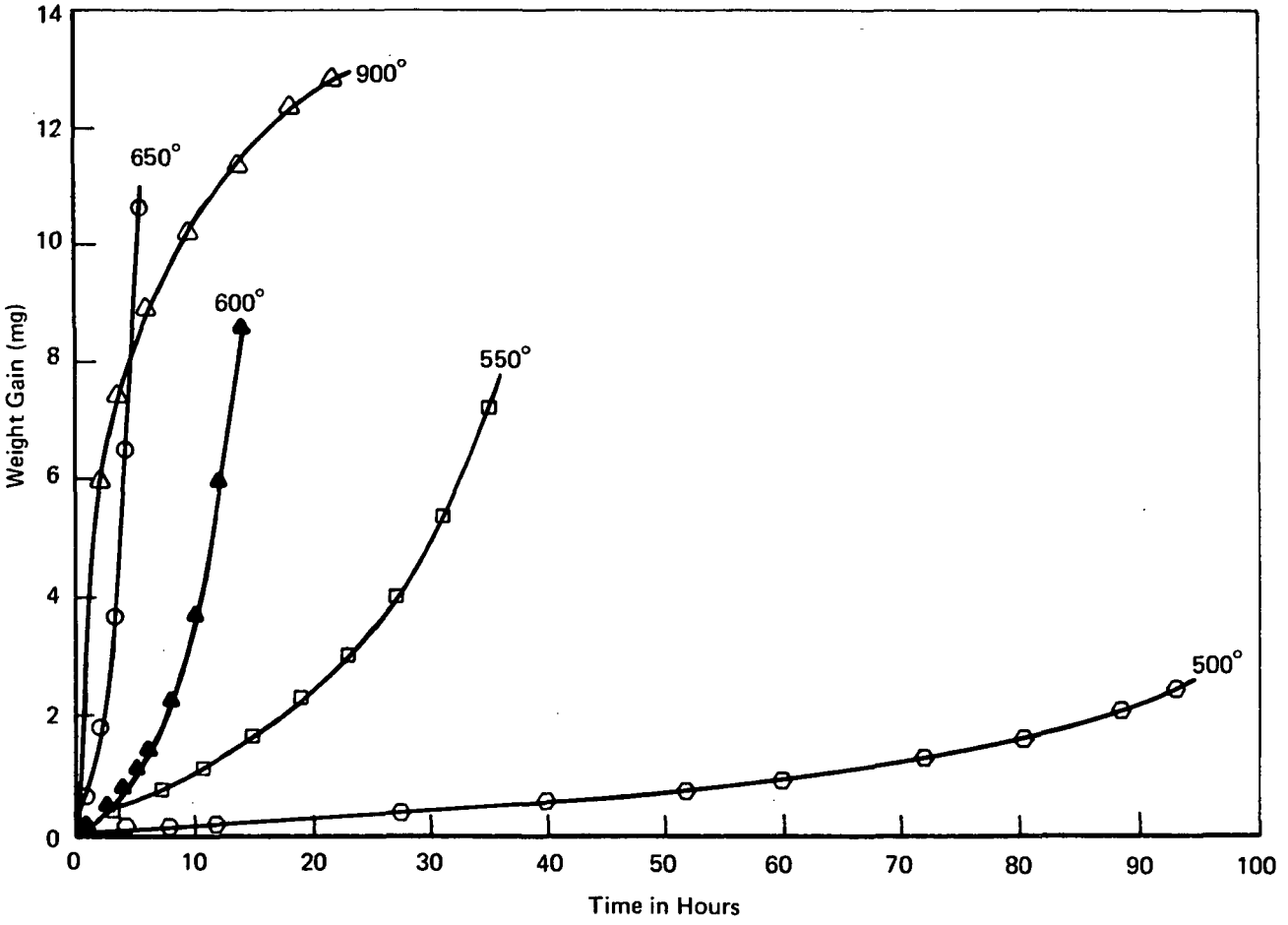

FIGURE 3 OXIDATION OF $CbAl_3$ IN ONE ATM. OF OXYGEN

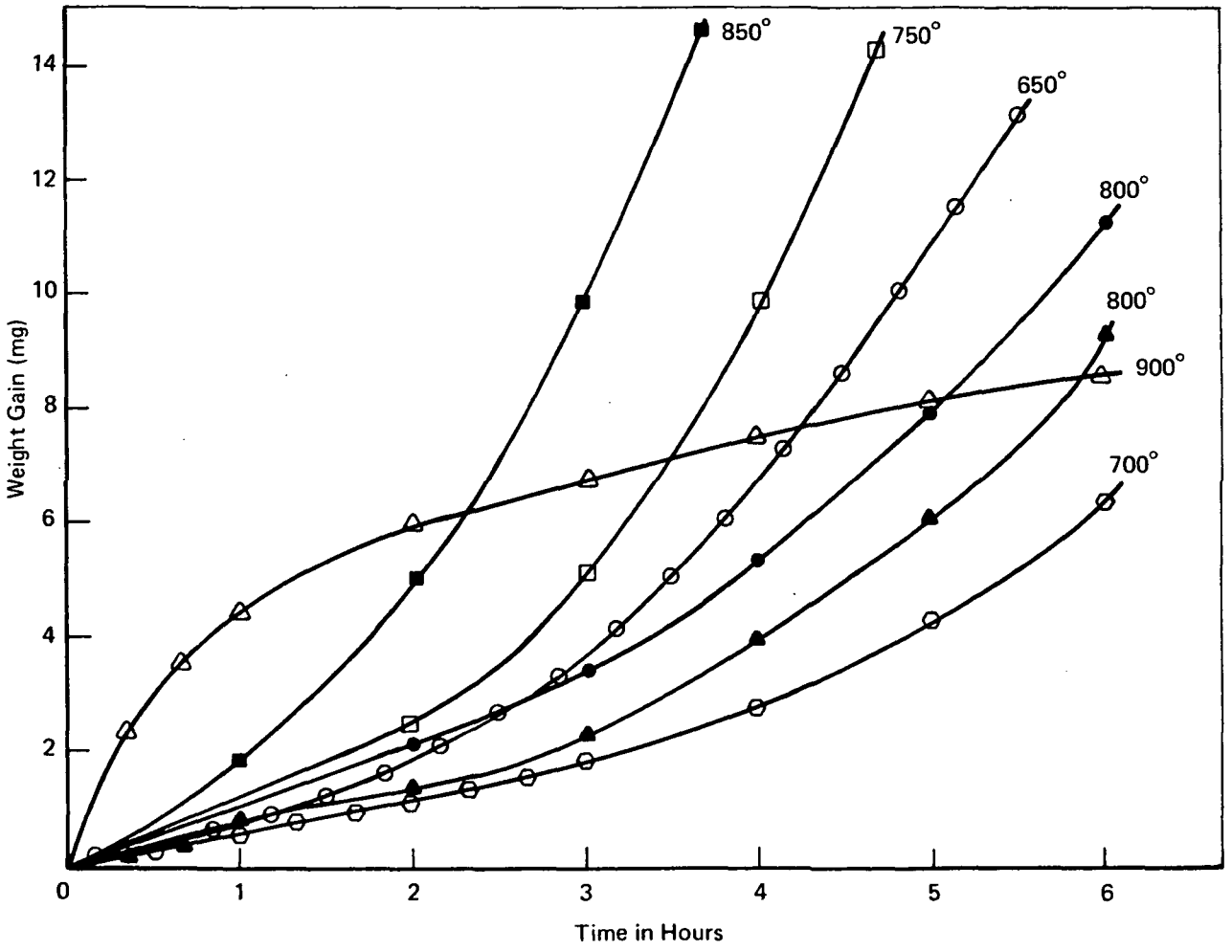

FIGURE 4 OXIDATION OF $CbAl_3$ IN ONE ATM. OF OXYGEN

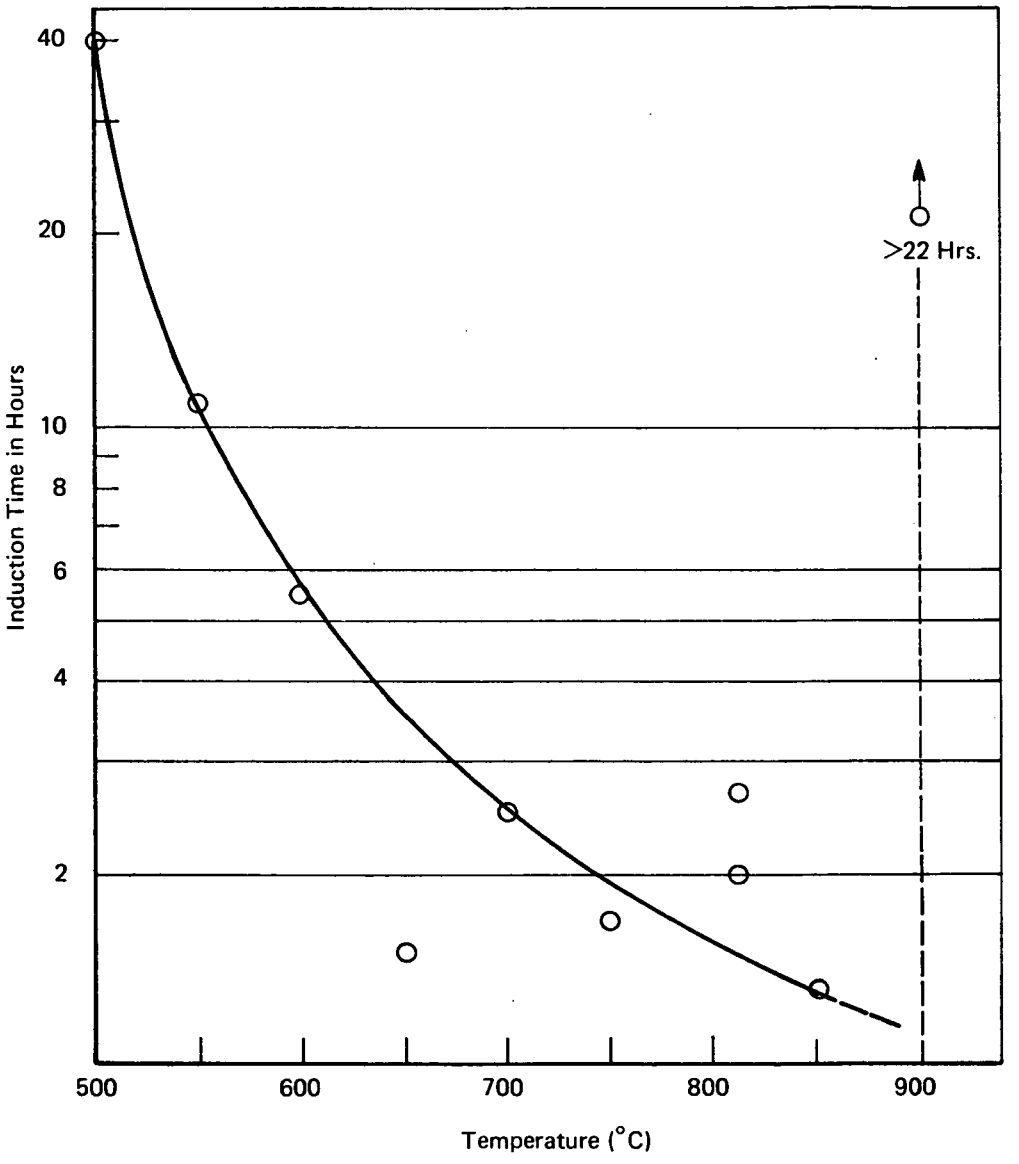

FIGURE 5 TIME TO INITIATE PESTING IN $CbAl_3$ IN ONE ATM. OF OXYGEN

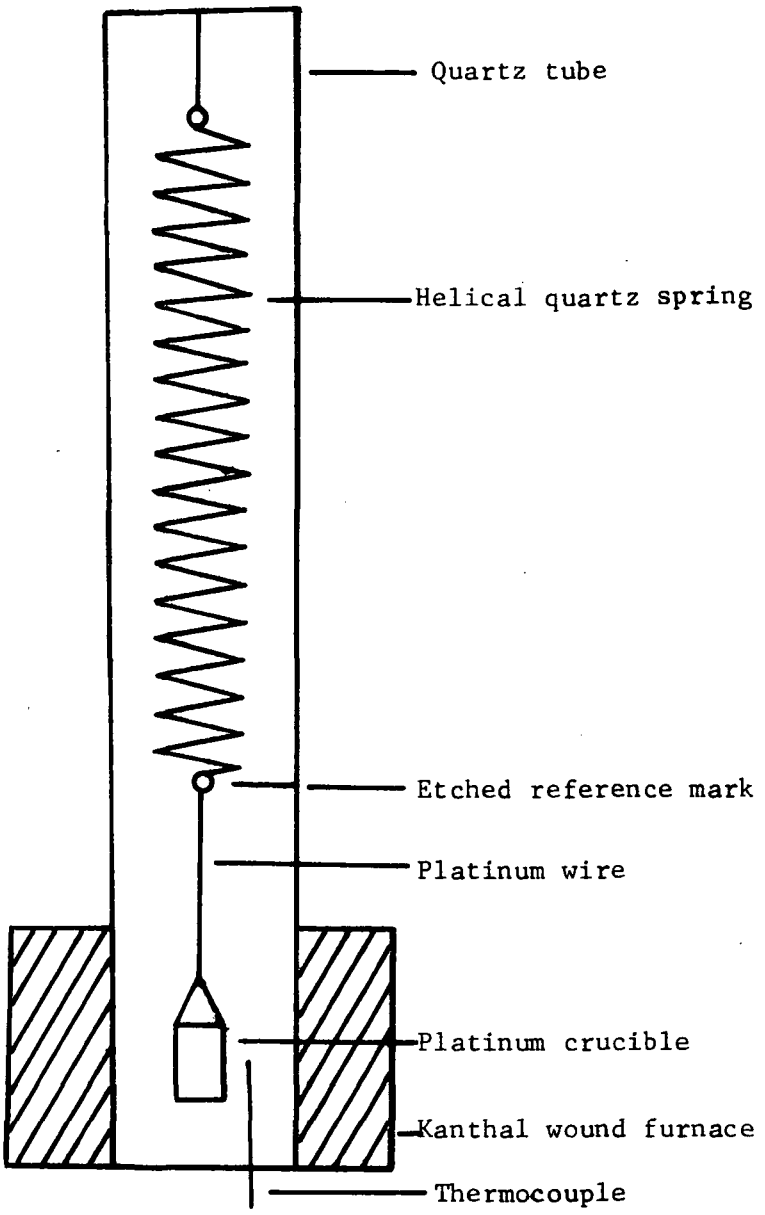

FIGURE 6 SCHEMATIC OF WEIGHT LOSS APPARATUS

of 10^{-5} grams. Results are shown in Figure 7. In contrast to the curves in pure oxygen, three regions can be distinguished in the curves at 700 and 825°C - an initial period of high oxidation rate, an intermediate period of negligible oxidation rate (plateau region), and a final period of break-away oxidation. All samples exhibited a pest type disintegration.

It is interesting to observe that X-ray analysis of the oxide formed below 900°C, in the pest range, shows a mixture of Nb_2O_5 and Al_2O_3. Above 900°C, where oxidation is protective, only αAl_2O_3 has been found. (3), (4), (5)

D. Deformation of Polycrystalline $CbAl_3$

By analogy with results on $MoSi_2$, it might be expected that delayed failure times for $CbAl_3$ at a given S/S_N level would increase dramatically at 900°C, where a sharp transition from pest failure to protective oxidation occurs. Equipment limitations precluded experimental verification.

In $MoSi_2$ the transition to protective oxidation is gradual and is associated with the onset of plastic deformation. For comparison with $MoSi_2$, we investigated the deformation characteristics of polycrystalline $CbAl_3$ at 525°C and 725°C in compression. No deformation was observed at the lower temperature prior to fracture at a compressive stress of 36,300 psi. At 725°C, about 1/2 % deformation was put into the sample at a compressive stress level of 28,100 psi. Since neither delayed failure times nor weight change results indicate any decrease in the severity of the pest phenomenon until the oxidation mechanism changes it would appear that deformation characteristics alone cannot explain pest in $CbAl_3$. The delayed failure results suggest that a stress dependent step plays a role in the oxidation mechanism, but not necessarily a dominant or controlling role. The abrupt change at 900°C in the form of the oxidation vs. time curve, complete with a sharp transition from a mixed Nb_2O_5 - Al_2O_3 oxidation product to pure Al_2O_3, points to the importance of chemically controlled steps in the over-all oxidation mechanism. While it is fool-hardy to draw firm conclusions from activation

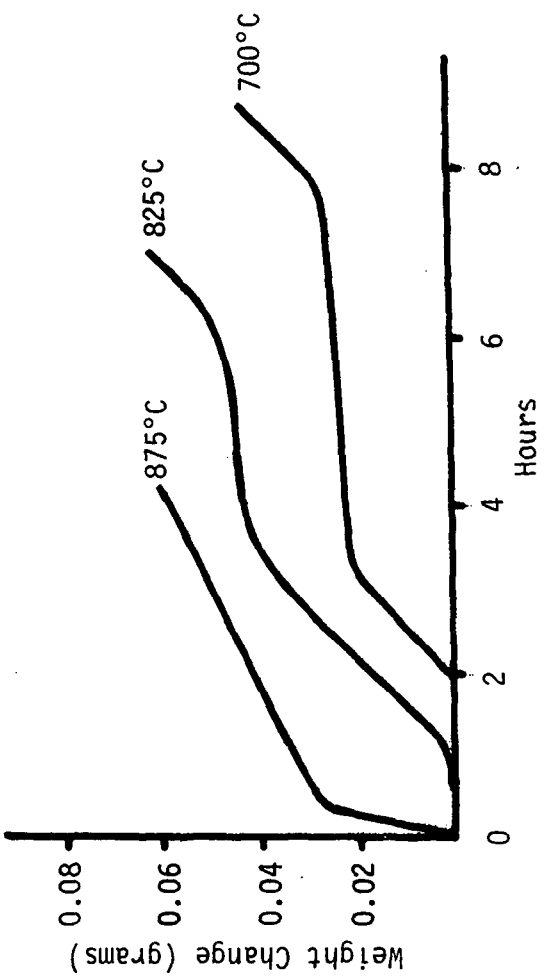

FIGURE 7 WEIGHT GAIN CURVE FOR POLYCRYSTALLINE COLUMBIUM ALUMINIDE

energy data, it might be noted that the empirically derived activation energy for delayed failure of 28.6 kcal/mole agrees well with the activation energy of 28 kcal/mole reported for diffusion of oxygen in Nb_2O_5 over the 500-1000°C temperature range. It is also close to the range of values 25 - 32.2 kcal/mole that have been found for diffusion of oxygen in niobium metal. [3] In contrast, the activation energies for diffusion of both oxygen and aluminum through Al_2O_3 are very much higher. For self-diffusion of aluminum in Al_2O_3, the value is 114 kcal/mole at temperatures of 1670 - 1900°C; and for diffusion of oxygen, the activation energy is 152 kcal/mole above 1600°C and 57.6 kcal/mole below.

III. DEFORMATION IN MOLYBDENUM DISILICIDE

The increasing resistance of $MoSi_2$ to pest failure at temperatures above 500°C and the complete absence of pest above about 650°C has been ascribed to the fact that the material begins to deform plastically in this temperature range. One approach to elimination of pest failure is to provide a mechanism for deformation at lower temperatures. A study of the deformation characteristics of single crystal molybdenum silicide was included as part of the present program in order to provide a baseline for the development and testing of new pest resistant coating concepts. A parallel study was originally planned with $CbAl_3$, but no single crystal could be obtained.

A. Introduction

Previous work at Arthur D. Little, Inc.,[6] has shown that slip can occur at 600°C on the {103} < 101 > system. This system was identified by analysis of deformation in single crystals of $MoSi_2$ deformed in tension. In addition, Vahldieck and Mersol[7] have shown by examination of slip traces near hardness indentations in single crystal $MoSi_2$ that slip occurs on the {100} and {110} planes. These authors suggest a possible slip direction, the [001], which is common to both planes but do not offer proof for this direction. Thus, there are gaps in identification of the slip systems, and little is known about the deformation characteristics as a function of temperature and crystallographic orientation.

B. Experimental

Single crystals of molybdenum disilicide were prepared by a floating zone crystal synthesis technique that had been developed earlier in this laboratory. Briefly, the procedure consists of mixing 200 mesh molybdenum disilicide powder of 99.5% purity with 2% weight silicon powder of 99.99% purity. This excess silicon is added to compensate for evaporative losses during crystal synthesis. This powder mixture is then packed in 3/8" diameter die by ramming the mix into the die. The powders are then sintered by heating to 1300 $\pm$ 10°C for three (3)

hours in a flowing argon atmosphere and then allowed to cool in the furnace under this protective atmosphere. These sintering conditions produce a compact which is approximately 85% dense, which for this material is ideal for growth by the floating zone technique. The sintered rod measures approximately seven (7) inches in length and 3/8" in diameter. A molten zone is passed up along the length of the sintered rod at a rate of one (1) inch per hour by means of an induction coil. A ceramic tube which contains a molybdenum radiation shield is suspended from the induction coil. It was found that this shielding system reduces thermal gradients in the as-grown crystal as it cools, thus preventing the formation of cracks. A flowing argon-5% hydrogen atmosphere is maintained in the chamber during crystal growth.

Rectangular bar specimens were cut from single crystal boules using a spark discharge machine. These bars, which measured approximately 0.20 cm x 0.20 cm x 0.50 cm, were lapped on 600 grit silicon carbide paper and then polished on a 6-micron diamond lap. These specimens were subsequently deformed in compression along the long axis with an Instron testing machine. The deformation experiments were carried out in a tungsten resistance heated-high vacuum furnace which is mounted on the Instron testing machine. Deformation experiments were carried out at temperatures between 625°C to 1125°C and a vacuum of 10^{-5} torr. Crystals were strained between 2-5% at a strain rate of 1×10^{-2}/min.

After deformation the slip planes were determined by two independent techniques. In one, the slip plane was identified by the orientation of the traces on the specimen surfaces. Prior to deformation, the side faces were lapped and polished. The orientation of the top cross-sectional face was determined by back reflection Laue patterns. From the crystal orientation and slip trace orientations, the slip plane was determined by analysis of the corresponding stereographic projection. In the other technique, the crystal was mounted on a goniometer and oriented so that a cut could be made parallel to the slip plane using the cutting wire of the spark discharge machine. After sectioning, the orientation of the slip plane was determined from analysis of a

back reflection Laue pattern.

Three crystals were tested and the poles of the stresses axes for the three orientations used in these experiments are plotted in Figure 8. In the first series (Series A) the top cross-sectional face is 11° from the (100) plane and 14° from the (101) plane, the second series (Series B) 18° from the $(0\bar{1}0)$ and 11° from the $(0\bar{1}1)$ plane, and the third series (Series C) 20° from the (100) plane and 20° from the (101) plane.

These orientations were obtained by cutting a single crystal boule approximately parallel to (Series A), perpendicular to (Series B), and at an angle to (Series C) (the growth axis of the crystal). In view of the fact that the growth direction was parallel to the $\vec{a}$ direction, the perpendicular cut (Series B) has almost the equivalent orientation as Series A. We have plotted the equivalent stress axis pole for Series B in Figure 8 as b*.

For each of the three orientations, Series A,B, and C, slip was found to occur on the 110 plane. As mentioned previously, 110 slip has been noted by others but the slip direction which operates in this plane had not been identified. In this study the deformation was in compression, and it is not possible to identify the slip direction from rotation of crystallographic planes as in tensile tests. Calculation of the resolved shear stresses on known and postulated slip systems was used to identify a probable slip direction.

The Schmidt factor (τ/σ) i.e., the ratio of the applied stress resolved on an assumed slip system, was calculated for reported and other probable slip systems to help identify the probable slip direction. The results of these calculations for the stress axes used in series A,B, and C are given in Table I for the {100} <0017 and {110} <001> slip systems reported by Vahldieck and Mersol[7] the {103} <101> slip system previously reported by ADL; the {110} <110> slip system which is a theoretically possible slip system in the observed slip plane. Comparison of the τ/σ's for <001> and <110> slip directions on the observed {110} slip plane indicates that <110> slip is more likely provided critical

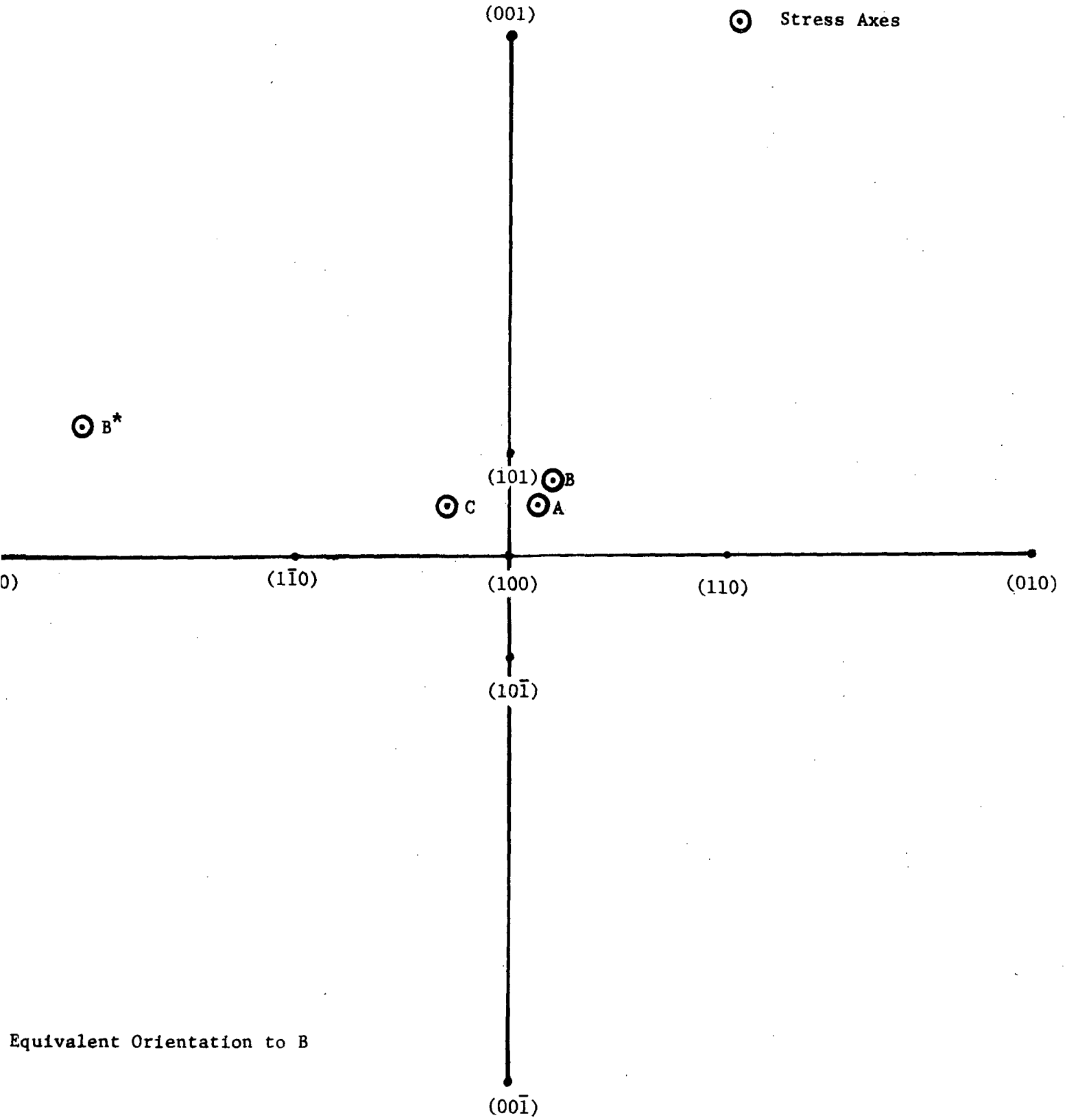

FIGURE 8 ORIENTATION OF STRESS AXIS

TABLE I

Critical Resolved Shear Stress Factor (τ/σ) for Various Slip Systems as a Function of Orientation

	SLIP SYSTEM		τ/σ	ORIENTATION
Source	Slip Plane	Slip Direction		
Postulated	{110}	<110>	0.47	
Reference 2	{110}	<001>	0.16	
Reference 2	{100}	<001>	0.20	(Series A)
Table I	{103}	<010>	0.09	
Postulated	{110}	<110>	0.43	
Reference 2	{110}	<001>	0.20	
Reference 2	{100}	<001>	0.25	(Series B)
Table I	{103}	<010>	0.12	
Observed	{110}	<110>	0.40	
Reference 2	{110}	<001>	0.08	
Reference 2	{100}	<001>	0.16	(Series C)
Table I	{103}	<010>	0.23	

resolved shear stresses are equal. These calculations also showed that {110} <110> slip systems were much more highly stressed than either {100} <011> or {103} <001> slip systems and thus the absence of the latter systems operation is not anomalous.

A comparison of the length of the minimum repeat distances in the <001> and <110> directions of the $MoSi_2$ lattice (c/a = 2.46) is a further indication that slip actually occurs in the <110> direction. Ignoring the dislocation core energy, the energy per unit length of a dislocation is proportional to $\vec{b}^2$. Thus, a <110> Burgers vector is energetically favored over a <001> Burgers vector by three times, $(E_{110} \approx \frac{2\,c^2}{(2.46)^2} \approx \frac{c^2}{3})$.

The experimentally observed yield stresses resolved on the {110} <110> slip system (Table II) are plotted in Figure 9 as a function of temperature. Within the experimental error, the data points for all three crystal orientations are presented by the same monitonic curve. The agreement between the calculated resolved yeild stresses for the A and B series with those of the C series is a further indication of the correctness of the identified slip system.

We believe that these three independent observations (τ/σ, Burgers vector length and consistent temperature dependence) are sufficient to conclude that slip occurs in the <110> direction on the <110> plane in $MoSi_2$. We recognize that direct identification of the Burgers vector by transmission electron microscopy or X-ray topography remain the only absolute proofs of this conclusion,

The onset of yielding was typically characterized by a sharp yield drop at all temperatures. The temperature dependence of the yield stress was described by an exponential function as shown by the log σ vs. log 1/T plot of the data in Figure 10. Interpretation of these characteristics requires knowledge of the initial number of mobile dislocations, the dependence of dislocation velocity on stress, the multiplication rate, the temperature dependence of the drag forces on the dislocations (both edge and screw components) as well as several experimental conditions such as testing machine stiffness and strain rate.

TABLE II

Critical Resolved Yield Stress Versus Temperature

	Critical Resolved Shear Stress		Temperature °C
	psi	kg/mm^2	
Series A	4896	3.45	1125
	5280	3.72	850
	8160	5.75	760
	10,700	7.54	650
	10,315	7.27	625
	10,512	7.41	625
Series B	4936	3.48	1000
	7994	5.63	750
	11,943	8.41	650
Series C	4810	3.38	1160
	5100	3.58	900
	13,100	9.23	625

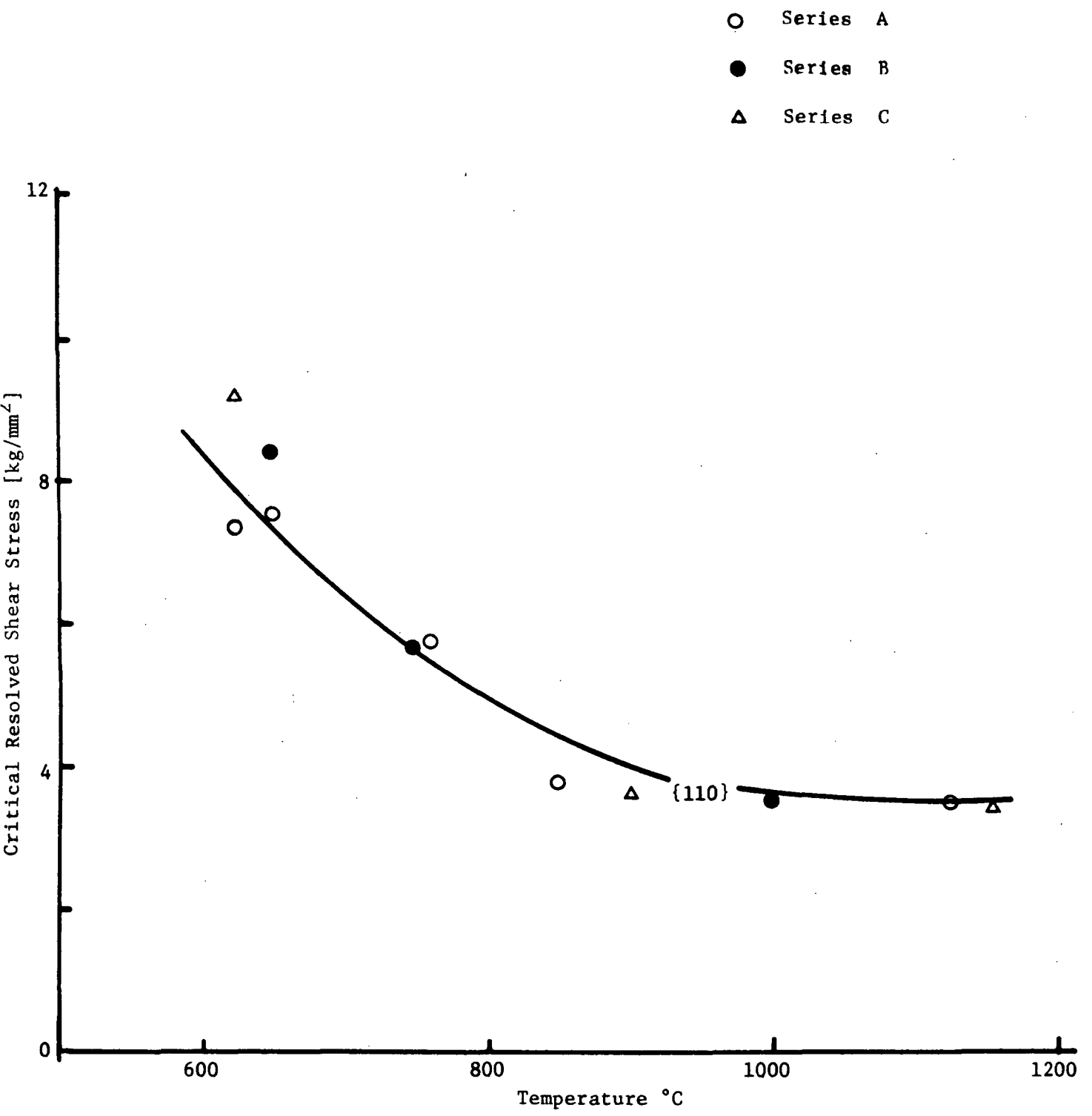

FIGURE 9 CRITICAL RESOLVED SHEAR STRESS AS A FUNCTION OF TEMPERATURE FOR SINGLE CRYSTAL $MoSi_2$

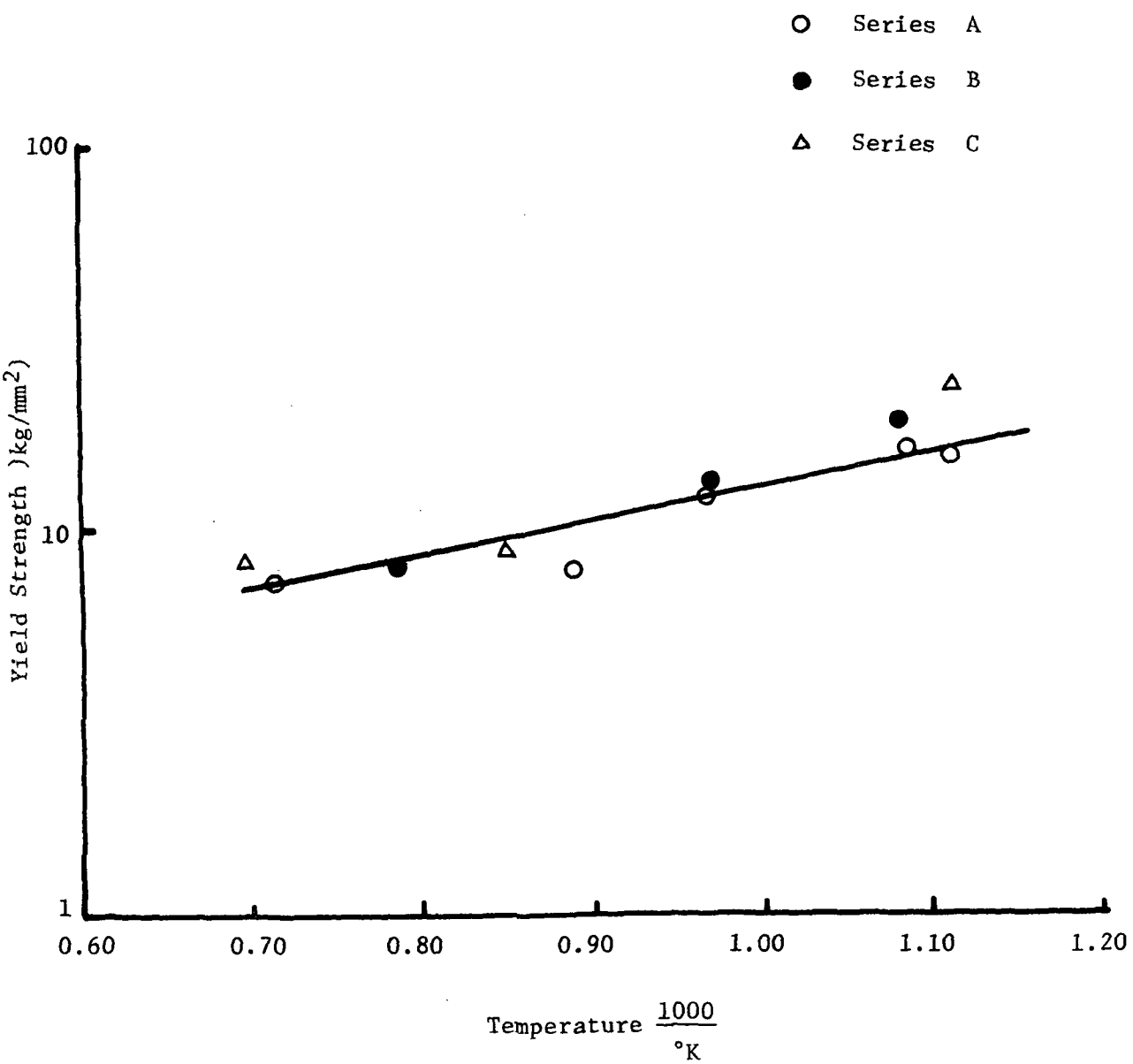

FIGURE 10 YIELD STRENGTH VERSUS TEMPERATURE

Dislocation densities in the as-grown crystals were of the order of $10^4/cm^2$. Transmission electron microscopic characterization substantiated the dislocation densities calculated by counting etch pits, since many thin sections were examined without observing dislocations. Low dislocation densities ($\leq 10^5/cm^2$) are known to be an important contributing factor in producing a yield drop.[8] The characterization procedures required to further clarify this phenomena were not undertaken in this program.

Dynamic creep measurements were made with crystals having {100} stress axes (A series). Samples were deformed at constant temperature and cross head rate until the stress reached a constant value, characteristic of that strain rate and temperature. The cross head rate was then progressively increased to establish the strain rate dependences of the steady state creep stress. Separate samples were used for each temperature. Corrected sample lengths and cross sectional areas were used to calculate actual strain rates and stresses.

The results of these creep measurements are plotted in Figure 11 for the three temperatures investigated. The slopes of all three curves indicate that for the steady state creep process

$$E = \sigma^5 e^{-Q/RT}$$

It has been shown[9] that this fifth order stress dependence is characteristic of a "dislocation-climb" stress relaxation (or recovery) process. Similar results have been observed in other single crystal samples when other grain boundary deformation processes are absent. A "dislocation-climb" recovery process is most likely to be operative when dislocations are not extended into partials since their recombination is not required to climb past stress fields which impair their motion. The individual dislocations and dislocation nodes which have been examined by transmission electron microscopy showed no evidence of stacking faults or extension into partials. These observations support the conclusion that recovery occurred by a dislocation climb process.

The apparent activation energy (Q) was calculated for the creep data shown in Figure 11. The temperature range and number of data points are limited so there is considerable uncertainty in this calculation. At a stress level of 14 kg/mm^2, the effective activation energy is in the range of 16 to 19 kcal/mole. This result is anomalously low. The activation energy for a creep process which is controlled by dislocation climb should be nearly equal to that of the self diffusion coefficient for the rate controlling ion. The activation energies for the self diffusion coefficients of Mo and Si in $MoSi_2$ have not been reported; however, the activation energy for Si diffusion in Mo_5Si_3[10] is 86 kcal/mole while for Si diffusion in Mo_3Si[10] it is 78 kcal/mole. It would be expected that the self diffusion coefficient activation energy for Mo would be larger since its ionic radius exceeds that of Si. On the basis of these results, the apparent activation energy for the creep process in single crystal $MoSi_2$ is approximately an order of magnitude smaller than would have been expected based on results with other materials. We have no explanation for this anomaly.

Steady state creep could not be established with B and C orientation samples. This is difficult to understand since the A and B series should be nearly equivalent from the standpoint of deformation processes.

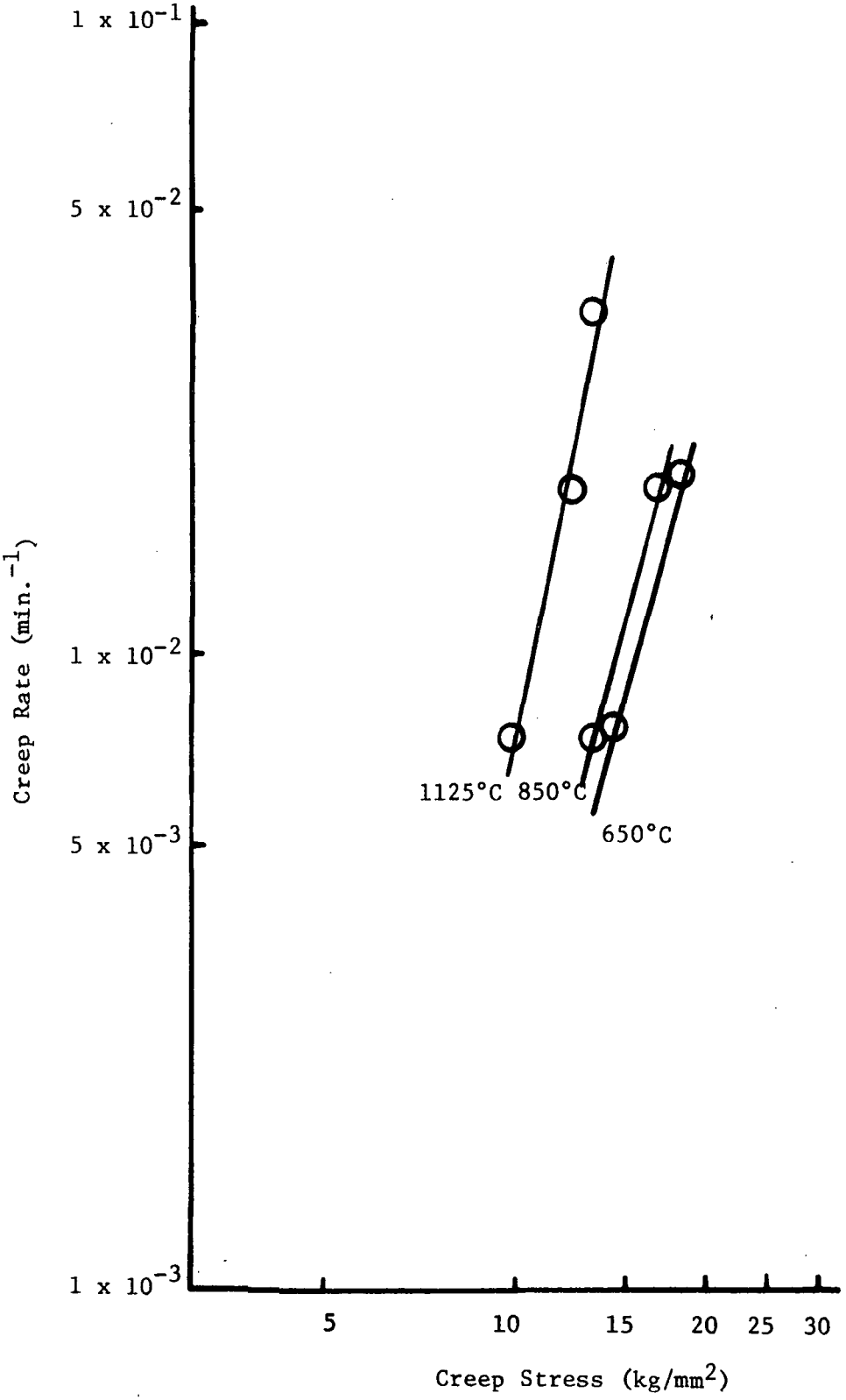

FIGURE 11 CREEP RATE VERSUS CREEP STRESS FOR SINGLE CRYSTAL $MoSi_2$ AT THREE TEMPERATURES

REFERENCES

1) J.B. Berkowitz-Mattuck, M. Rossetti, and D.W. Lee, Metallurgical Trans. 1, 481 (1970).

2) A.V. Seybolt and J.H. Westbrook, Technical Documentary Report No. ASD-TDR-63-309, Part I, April,1963.

3) Per Kofstad, "High Temperature Oxidation of Metals," John Wiley and Sons, N.Y. (1966).

4) L. Sama, Tech-Document. Rept. No. ASD-TDR-63-160, February, 1963.

5) D.D. Lawthers and L. Sama, ASD Tech. Rept. 61-233, October, 1961.

6) Final Report, "The Pest Phenomenon in Intermetallics," NASW-1403, August, 1968.

7) F.W. Vahldiek and S.A. Mersol, "Phase Relations and Substructure in Single Crystal $MoSi_2$," J. Less Common Metals, 15, pp. 165-176 (1968).

8) W.G. Johnston, "Effect of Impurities on the Flow Stress in LiF Crystals," J. Appl. Phys. 33, 2050-58 (1962).

9) J.R. Weertman, "Steady-State Creep through Dislocation Climb," J. Appl. Phys. 28, [3] 362-64 (1957).

10) R.W. Bartlett and P.R. Gage, Technical Documentary Report No. ASD-TDR-63-753, Part II, July, 1964.

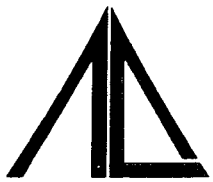

CAMBRIDGE,
MASSACHUSETTS

CHICAGO
NEW YORK
SAN FRANCISCO
WASHINGTON
ATHENS
BRUSSELS
CARACAS
LONDON
MEXICO CITY
PARIS
RIO DE JANEIRO
TORONTO
ZURICH